Materials Research Proceedings 54 (2025) 2281-2290 https://doi.org/10.21741/9781644903599-246

Mechanical and kinetic characterization of additively manufactured PLA structures for improved process and warpage modeling

Felix Frölich[1,a *], Dominik Dörr[2], Alexander Jackstadt[1], Florian Wittemann[1] and Luise Kärger[1,b*]

[1]Karlsruhe Institute of Technology (KIT), Institute of Vehicle System Technology (FAST), Lightweight Engineering, Rintheimer Querallee 2, Karlsruhe, 76131, Germany

[2]SIMUTENCE GmbH, Rintheimer Querallee 2, Karlsruhe, 76131, Germany

[a]felix.froelich@kit.edu, [b]luise.kärger@kit.edu

Keywords: Material Extrusion, MEX, Material Modeling, DSC, DMA, TMA

Abstract. This work focuses on the kinetic and thermomechanical characterization of a polylactide (PLA) in the context of material extrusion (MEX) to gain a basis for material modeling that can be utilized to predict process-induced deformations throughout the process chain using process simulation. The research provides a detailed understanding of the material behavior at different process stages and the mechanisms contributing to residual stresses and warpage. This is achieved through experimental investigations using differential scanning calorimetry (DSC), dynamic mechanical analysis (DMA), and thermomechanical analysis (TMA). In order to cover each process step, the experiments are performed on printed and partly on raw material. Finally, the discussed results are summarized in a recommendation as to which effects should be considered in each process step for adequate warpage prediction.

Introduction

Additive manufacturing (AM) technologies offer the potential for significant cost savings by reducing material waste and enabling tool-less production of complex geometries. One widely used technology is material extrusion (MEX). The following steps outline a typical additive manufacturing process chain: Once the component is designed, it gets divided into individual layers and the nozzle trajectory within these layers is defined. The information about the nozzle trajectory and the process parameters is transferred to the printer as a G-code. The firmware interprets the code according to printer-specific constraints, such as possible nozzle acceleration or cornering. The printer builds the component layer by layer by extruding a polymer melt through a nozzle. The component is then detached from the build plate and any supporting structures are removed. The printed components can also be annealed to increase the degree of crystallinity and the strength of the interface between the layers, thereby increasing the strength of the entire component.

Among many commercially available thermoplastics as feedstock, polylactide (PLA) is widely used in the MEX process due to its biodegradability, environmental compatibility, and good processability. However, due to limitations in mechanical and thermal properties, PLA components are limited to prototyping and basic applications, so post-treatment by annealing expands the range of possible applications [1,2]. However, the MEX process and the subsequent post-treatment can lead to warpage problems which may prevent the components from being used. Numerical methods can be a helpful tool to gain insight into the development of residual stresses and warpage and to understand the complex interactions involved in producing complex components with the highest possible strength.

Process simulation: Several approaches have been published to predict process-related heat distribution and the resulting warpage in the MEX process. The problem is usually solved using

finite element approaches. Zhang and Chou [3] developed an approach to simulate heat transfer. They represent the material extrusion process by activating elements according to the nozzle trajectory. Other authors [4-6] use the same approach to predict process-induced warpage using a sequentially coupled thermomechanical approach. In the publication by Trofimov et al. [6] on modeling process-induced warpage, PLA is used as the filament material.

Characterization: Trofimov et al. derive the experimentally determined material properties from Farah et al. [7] and Espinach et al. [8]. Both studies show extensive experimental investigations of the material behavior, but without considering the influence of the process-typical mesostructure. Espinach et al. show results of differential scanning calorimetry (DSC) measurements, dynamic mechanical analysis (DMA), thermal gravimetric analysis (TGA), and thermo-mechanical analysis (TMA) and thus provide a foundation for understanding mechanisms within PLA, that can lead to warpage during a manufacturing process. An overview of the dynamic mechanical behavior, the crystallization kinetics, and the quasi-static behavior of various bioresorbable PLAs is also provided by Bergström and Hayman [9]. In addition, there are various publications in the context of crystallization kinetics [10,11] and the dynamic mechanical behavior [12] of PLA, but these are concerned more with various modifications of PLA or the influence of different fillers and not with additively printed structures. Some experimental studies have also been published on the influence of the MEX process on the above-mentioned material properties: Srinivas et al. [13] investigate the absolute crystallinity of printed structures in different layers, with the result that amorphous structures occur at a height of 2.5 mm. The influence of the process-typical mesostructure and the underlying process parameters on the dynamic-mechanical behavior of PLA [14] and other thermoplastics [15,16] has also been investigated. The influence of the mesostructure on the quasi-static behavior of printed PLA is shown in several papers [17,18] and modeled in others [19,20].

The state-of-the-art shows in various works the complex behavior of crystallization kinetics and thermomechanical behavior of PLA. The mesostructure induced by MEX has an additional influence on these material properties. Therefore, it is important to consider this process-property relationship in the numerical modeling of the MEX process. In the literature, however, this special process-property relationship has not yet been linked to the necessary material modeling for simulating the entire process chain. Hence, the present work deals with the question which process-specific material properties of PLA occur in which process step and should be modeled. This is discussed based on experimental investigations using differential scanning calorimetry (DSC), dynamic mechanical analysis (DMA), and thermo-mechanical analysis (TMA). Due to the extensive literature in this area, investigations of quasi-static behavior are not presented. To cover each process step, the experiments are performed on printed and partially on raw material. Finally, the discussed results are summarized in a recommendation on which effects should be considered in the individual process steps.

Methods

Material. The material used is the commercial Ultrafuse polylactide (PLA) filament from BASF [21]. The material properties listed in Table 1 are given in [21].

Process. The Ultimaker 2+ was used to produce the test specimens in this paper. The standard glass print bed has been replaced by a FilaPrint print bed from Filafarm. The nozzle used has a diameter of 0.4 mm and was specified with a print resolution of 200 µm to 20 µm. The slicer and printer settings, listed in Table 2, were selected based on printing studies to achieve a consistent and reproducible microstructure. The fan was switched on from the second layer on.

Materials Research Proceedings 54 (2025) 2281-2290 https://doi.org/10.21741/9781644903599-246

Table 1 – Material properties of BASF Ultrafuse PLA filament [21]

Material properties	Value	Unit
Density ρ	1248	$\mathrm{kg \cdot m^{-3}}$
Glass transition temperature T_g	60	°C
Melting temperature T_M	151	°C
Processing temperature T_proc	210-230	°C

Table 2 – Slicer and process parameters selected for the manufacturing of all specimens

Process parameter	Value	Unit
Nozzle temperature T_N	210	°C
Bed temperature T_bed	60	°C
Layer height l_heigth	0.2	mm
Extrusion width e_width	0.4	mm
Printing speed v_p	50	$\mathrm{mm \cdot s^{-1}}$

Specimen preparation. To exclude manufacturing influences, such as the perimeter or the turning points of the deposited polymer strands, our previous investigations on suitable mechanical properties characterization [17] were utilized. The specimens were cut out of an additively manufactured plate according to the specifications in [17]. The dimensions of the specimens are described in the respective subsections of the individual characterization tests.

Dynamic Mechanical Analysis (DMA). A DMA was performed at 1 Hz to determine the relative influence of temperature on stiffness. In the context of this work, this was carried out on a specimen with a structure oriented in the direction of loading (0°). The influence of the strand orientation is not considered in this work. This is based on the assumption that the influence of orientation on the temperature dependence of the stiffness of PLA is comparatively small and can therefore be neglected, which has been confirmed in preliminary experiments. An Instron E3000 ElectroPuls^{TM} with a nominal force of 3 kN and a load cell capacity of 5 kN was used. The machine was equipped with an Instron liquid nitrogen-cooled temperature chamber. To protect the load cell from overheating during the test, a water-cooling system was used to ensure accurate force measurement. Rectangular specimens with a length of 160 mm, a width of 10 mm, and a thickness of 3 mm were used. The clamping on both sides was 50 mm, resulting in a free specimen length of 60 mm. A temperature range of 25 °C to 145 °C was measured with isothermal steps of 2.5 °C. The specimens were loaded with a mean strain of 0.25 % and a strain amplitude of 0.125 %. This loading is within the linear viscoelastic region.

Thermomechanical Analysis (TMA). The key factor for warpage mechanisms in the process chain is the volume change due to temperature changes. The solid mechanics modeling of the printing process and the study of the reheating during the annealing process make it necessary to determine the volume change of the printed structures and not of raw material. Therefore, a TMA was performed to characterize the changes in length. The TMA/SS-6000 from Seiko Instruments was used. The investigations were carried out on cubic specimens with a uniform edge length of 6 mm. Specimens were prepared with unidirectional orientation of the deposited strands to examine the change in length along (0°) and across (90°) the extrusion direction. The specimens were printed with a nozzle diameter (d_N) of $d_\mathrm{N1} = 0.4\,\mathrm{mm}$ and $d_\mathrm{N2} = 0.8\,\mathrm{mm}$, respectively. Furthermore, the specimens were annealed to separate the irreversible effects during this process step. The heating rate was 1 K/min, and the applied preload was 20 mN.

Differential Scanning Calorimetry (DSC). Material-specific crystallization kinetics are an important factor in the formation of component warpage in the process chain. Crystallization effects lead to volume changes and the degree of crystallinity influences the stiffness of the material. DSC measurements are used to characterize the kinetics and to determine which crystallization effects occur at which stages of the process. To account for the full history of the PLA, the crystallization behavior during cooling from the melt (extrusion from the nozzle) and during heating of the additive manufactured structures (annealing) is performed. For cooling from the melt, cooling rates of 5 K/min, 10 K/min, 20 K/min, 30 K/min, 40 K/min and 50 K/min were investigated. It should be noted that much higher cooling rates can occur during the printing

process. To assess the absolute crystallinity χ_c of the specimens after cooling, they were reheated at a rate of 10 K/min. The absolute crystallinity χ_c in different specimens can be calculated by:

$$\chi_c = \frac{\Delta H_m - \Delta H_{cc}}{\Delta H_m^\circ} \times 100\ \%, \quad (1)$$

where ΔH_m is the absolute melting enthalpy, ΔH_{cc} is the absolute cold crystallization enthalpy, and ΔH_m° is the absolute melting enthalpy of 100 % crystalline PLA that is 93 $J \cdot g^{-1}$ [22]. To increase the validity of the data, two measurements were made for each cooling rate.

To investigate the kinetics of additively manufactured structures, specimens are taken from printed plates and heated at 0.5 K/min, 1 K/min, 5 K/min, 10 K/min, and 20 K/min. To determine the absolute crystallinity χ_c of the printed plate, the initial absolute crystallinity was determined based on the enthalpy changes during the heating process.

As part of these investigations, two measurement campaigns were carried out. The first with cooling rates of 1 K/min - 10 K/min with two measurements each. A second was performed at 0.5 K/min and 20 K/min with three measurements each to cover a wider range of heating rates occurring during annealing. To ensure comparability of the two sets of measurements, an additional measurement at 1 K/min was made during the second campaign and compared with those of the first campaign. The enthalpy change during cold crystallization and melting was used as a comparative measure. The first set of measurements gave an average enthalpy change of $\Delta H_{cc} = 21.21\ J \cdot g^{-1}$ during cold crystallization and $\Delta H_m = 23.01\ J \cdot g^{-1}$ during melting. The second set of measurements gave an average enthalpy change of $\Delta H_{cc} = 20.90\ J \cdot g^{-1}$ during cold crystallization and $\Delta H_m = 23.61\ J \cdot g^{-1}$ during melting. The comparison shows that the two sets of measurements are comparable and can be combined for investigation.

To investigate the influence of the typical mesostructure on the crystallization behavior, the enthalpy changes were compared when heating a printed structure and a previously melted and resolidified structure (unstructured) at a heating rate of 1 K/min. The comparison is made within a single measurement on a specimen with multiple heating and cooling phases. This ensures that the measurements are not subject to scatter between different series of measurements.

Results and Discussion

DMA. Fig. 1 shows the storage modulus E' as a function of temperature T. E' is significantly higher below the glass transition temperature $T_g = 62.4 \pm 0.3$ °C. At a temperature of 25 °C, the module is $E' = 2910$ MPa , and just above T_g it is $E' = 20$ MPa. From around 70 °C the stiffness increases to $E' = 150$ MPa before decreasing with increasing temperature. The 99.28% decrease in modulus shows the strong softening of PLA when T_G is exceeded. The increase of E' at higher temperatures is due to cold crystallization effects during the experiment. The visible cold crystallization effects also indicate that the initial absolute degree of crystallinity of the specimens was low. This may be due to the high cooling rates during the manufacturing process combined with PLA-specific slow crystallization kinetics. These hypotheses will be addressed in the discussion of the DSC experiments later in this work. For material modeling of PLA over the entire process chain, these results imply that during the printing process for $T > T_g$, the stiffness of PLA corresponds to the stiffness of a low degree of crystallinity. This is equivalent to the stiffness for a temperature just above T_g. However, the influence of the increasing degree of crystallinity on the stiffness during annealing must be considered.

TMA. Fig. 2 shows the change in length as a function of temperature as strain ε in %. The minimum and maximum values at each measurement point are shown in shaded colors. The blue line shows the change in length for specimens with a nozzle diameter of $d_{N1} = 0.4$ mm. The yellow line shows data for a nozzle diameter of $d_{N2} = 0.8$ mm. The solid lines illustrate the measurements in the extrusion direction (0°), and the dashed lines transverse to the extrusion

direction (90°). The lines with dots at the measuring points show the measurements on annealed specimens.

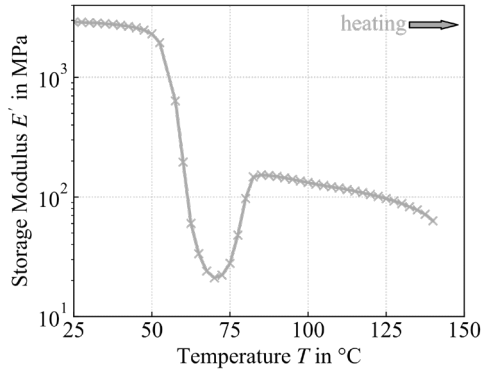

Figure 1 – Storage modulus E' as a function of temperature T, measured by DMA at a frequency of 1 Hz

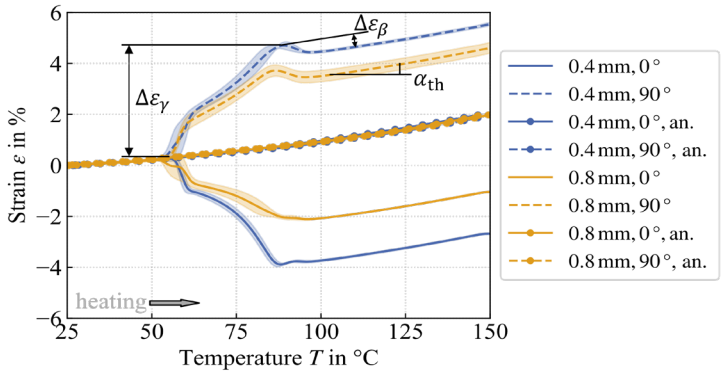

Figure 2 – Length changes with temperature as strain in %. Length changes with temperature as strain in % in extrusion direction (0°) and transverse to extrusion direction (90°)

When the temperature exceeds T_g there is a negative change in length in the extrusion direction and a positive change in length in the transverse direction for unannealed specimens. The behavior is affected by the nozzle diameter used, indicating that the effect is related to the shear strain in the polymer, which is affected by the nozzle diameter. The shear strain in the polymer stretches the molecular chains as they exit the nozzle. Due to the high cooling rates and nozzle motion, the chains do not reorient completely after exiting the nozzle and remain in an aligned state. When reheated above the glass transition temperature, the chains reorient to their energetically most favorable state, which is a ball-like form. This phenomenon is also referred to as entropic elasticity and results in the deposited strands becoming shorter on reheating but wider transverse to the extrusion direction. This change in length is irreversible and is labeled $\Delta\varepsilon_\gamma$ in Fig. 2. The slope below T_g and after the change in length due to entropic elasticity $\Delta\varepsilon_\gamma$ represents the thermal expansion coefficient α_{th}. This expansion is reversible, as shown by the same slope for the annealed specimens. In addition, a change in length due to cold crystallization effects can be observed. This is labeled $\Delta\varepsilon_\beta$ in Figure 2. DSC tests confirm the temperature range in which this effect occurs. The changes in length with increasing temperature of the annealed specimens show no significant dependence on the strand orientation. This allows the assumption that α_{th} can be modeled isotropically. In contrast, $\Delta\varepsilon_\gamma$ and $\Delta\varepsilon_\beta$ should be modeled anisotropically.

DSC: Cooling from the melt stage. Figure 3a shows the specific heat flow $\dot{q}$ of PLA during cooling at rates of -5 K/min, -10 K/min, -20 K/min, -30 K/min, -40 K/min and -50 K/min. The figure shows the mean of two measurements, with the minimum and maximum values for each measurement point shown in shaded form. The crystallization peaks are less pronounced compared to the measured $\dot{q}$, which is a first indication that no significant crystallization effects occur at these cooling rates during the MEX process. In Fig. 3b the mean $\dot{q}_n$ normalized to the cooling rate is plotted for the measured rates. The crystallization peak region is shown without the heat flow baseline. In defining the crystallization temperature range, it was assumed that no crystallization effects occur below 80 °C at the cooling rates used here. This is based on previous isothermal DSC measurements. The enthalpy change is small, especially at the higher cooling rates. Since much higher cooling rates occur in the MEX process, this is another indication that the absolute degree of crystallinity after the printing process is low.

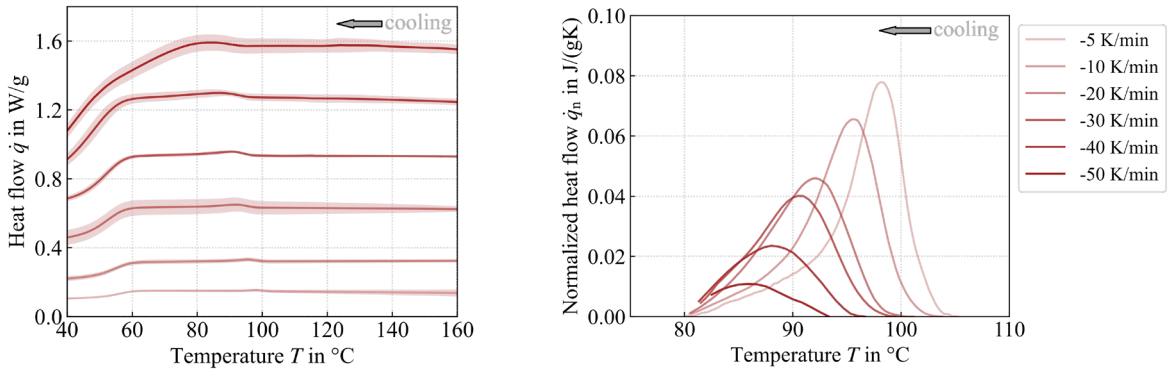

a) b)

Figure 3 – a): Specific heat flow $\dot{q}$ of PLA Ultrafuse during cooling at cooling rates of -5 K/min, -10 K/min, -20 K/min, -30 K/min, -40 K/min, and -50 K/min. b): Mean heat flow $\dot{q}_n$ normalized to the cooling rate for the measured rates. The area of the crystallization peak minus the baseline is shown

To further confirm this hypothesis, the measured specimens were reheated at a rate of 10 K/min and the changes in enthalpy ΔH during cold crystallization and melting were measured. Fig. 4 shows the specific heat flow $\dot{q}$ in the respective temperature ranges for cold crystallization (Fig. 4a) and melting (Fig. 4b). The enthalpy changes are much larger than for crystallization during cooling (Fig. 3b) and are not significantly different for all specimens. The initial degrees of crystallization in the specimens are therefore comparable, and it can be assumed that the initial degree of crystallinity must have been low.

DSC: Heating additively manufactured structures. Fig. 5a shows the specific heat flow $\dot{q}$ of printed PLA structures during heating at rates of 0.5 K/min, 1 K/min, 5 K/min, 10 K/min, and 20 K/min. The mean of two measurements per heating rate is shown, with the minimum and maximum values for each measurement point shown in shaded form. T_g appears as a peak in the range of 60 °C to 70 °C due to macromolecular organization and associated stress relaxation. Compared to cooling, the dependence of crystallization kinetics on the underlying heating rate is more pronounced during heating. Figure 5b illustrates the mean heat flow $\dot{q}_n$ normalized to the heating rate. The crystallization peak region is shown without the heat flow baseline. The measurements show the effect of the heating rate on the crystallization behavior of the printed structures. The enthalpy changes are higher compared to the cooling of the raw material. Hence, when modeling PLA in the annealing process step, crystallization effects and their influence on stiffness during heating must be considered.

The measurements can also be used to determine the initial absolute degree of crystallinity χ_c of the specimens using Eq. 1. Since the underlying specimens were cut from a printed plate, their degree of crystallinity provides information on the crystallization effects during the MEX process with PLA. A total of 13 specimens were measured and a mean absolute crystallinity of $\chi_c = 2.67\ \% \pm 1.28\ \%$ was determined.

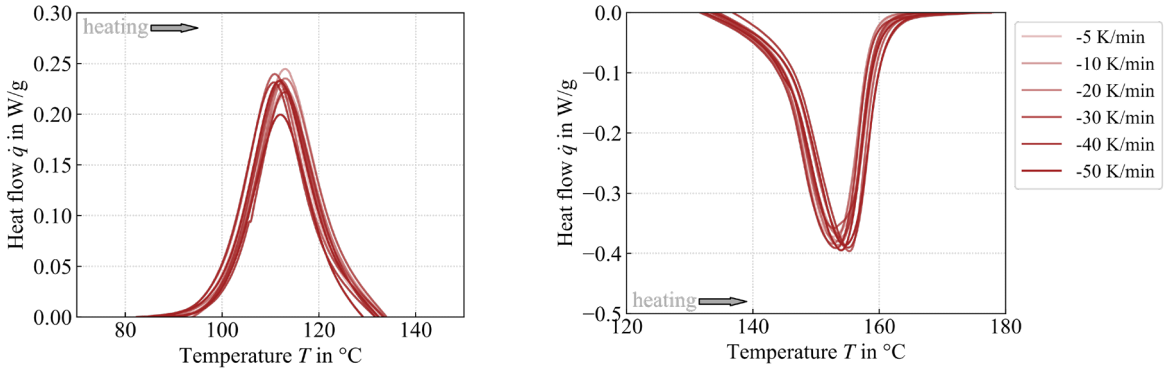

a) b)

Figure 4 – a) Specific heat flow $\dot{q}$ in the respective temperature ranges for cold crystallization and b) melting, resulting from heating the specimens previously cooled at different rates. The heating rate was 10 K/min for all measurements

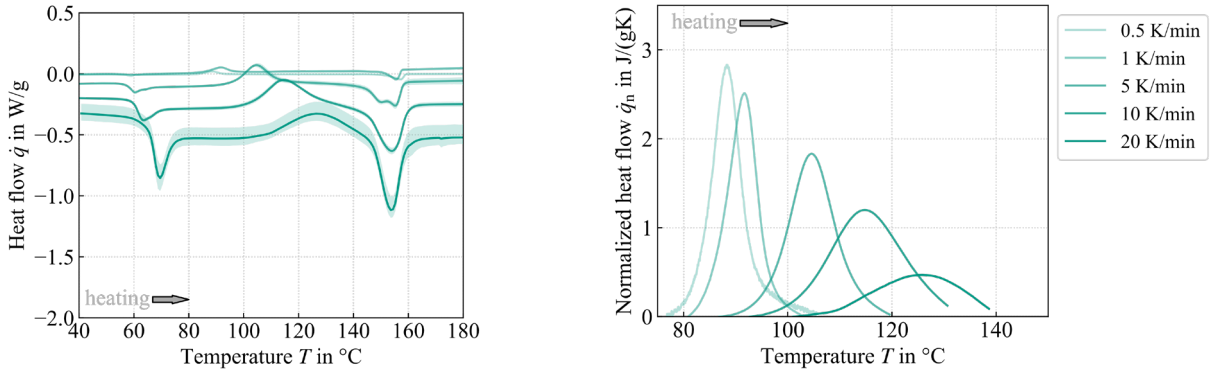

a) b)

Figure 5 – a): Specific heat flow $\dot{q}$ of PLA specimens printed with MEX during heating at rates of 0.5 K/min, 1 K/min, 5 K/min, 10 K/min, and 20 K/min. b): Mean heat flow $\dot{q}_n$ normalized to the heating rate for the measured rates. The area of the crystallization peak minus the baseline of the heat flow is shown

DSC: Heating comparison between printed and unstructured samples. Fig. 6 shows the comparison of the specific heat flow $\dot{q}$, when heating a printed structure, and a previously melted and resolidified specimen at a heating rate of 1 K/min. As described for Fig. 5a, T_g appears as a peak at about 60 °C due to the macromolecular organization. The peak is more pronounced in the printed structure, indicating higher solidified stresses. This supports the interpretation of the TMA results suggesting that the molecular chains solidify in a stretched state during the printing process. The measurements show that the process-specific printed structure influences the cold crystallization behavior. In printed structures, cold crystallization occurs at lower temperatures. Approximately between 80 °C and 105 °C for printed structures and between 90 °C and 110 °C for unstructured specimens. This may be due to the aligned molecular chains, which have fewer loops with neighboring molecular chains than the disordered structure and can therefore transform to the crystalline form more quickly. Hence, to characterize the crystallization behavior of PLA for modeling the annealing step using DSC, it is therefore necessary to study the kinetics based on the initial heating of printed specimens.

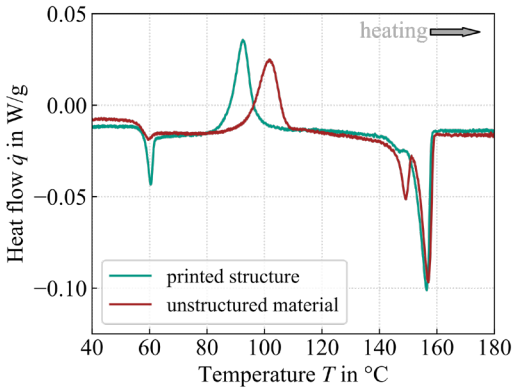

Figure 6 – Comparison of the specific heat flow $\dot{q}$ for a heating rate of 1 K/min of a printed structure in green and a previously melted and resolidified specimen (unstructured material) in red

Mechanisms to be modeled in the virtual process chain

The thermomechanical and kinetic characterization provides insight into the material properties of PLA and the mechanisms that occur in each phase of the MEX process chain (see Figure 1) that significantly trigger and shape the process-induced deformations. The identified mechanisms must be considered in material modeling if these deformations are to be predicted by numerical methods. The experimental investigations show that different mechanisms lead to or influence deformations in different process phases. It was found that crystallization effects during the printing process and the post-processing steps " detaching from the building plate " and " removal of support structures " can be neglected. The material modeling for the first three steps can therefore be identical and done without considering crystallization effects. The effects to be modeled up to the annealing process step are listed below:

- The 99.28% drop in the storage modulus indicates the pronounced softening of the PLA when the glass transition temperature is exceeded. The strong temperature dependence of the stiffness must be considered
- During the experiments on the additive manufactured structures, cold crystallization effects occurred. In conjunction with the measured absolute crystallization values of the structures, it can be assumed that no significant crystallization effects occur during the printing process. Therefore, they do not need to be considered in the material modeling up to the annealing process
- TMA experiments show that the resulting structure undergoes isotropic thermal expansion during the printing process. No molecular reorientation or cold crystallization occurs during the printing process. Anisotropic volume change due to molecular reorientation and cold crystallization therefore occurs only in a subsequent annealing step. Already annealed structures are therefore subject to isotropic thermal expansion again
- Additionally, previous work has shown that the material orientation induced by the trajectory leads to anisotropic stiffness [17,18]

Mechanisms to be considered when modeling the annealing process:

- When simulating the heating and annealing of printed components, in addition to the thermal dependence of stiffness, the dependence on the degree of crystallinity must be considered
- Cold crystallization effects depend on the heating rate. This rate dependency must be included in the material model when simulating heating and annealing. The crystallization kinetics for heating are to be characterized on printed specimens. The change in length of an extruded strand due to entropy elasticity and crystallization effects must be considered

Conclusion

As part of the simulative prediction of process-induced deformation in the material extrusion of PLA components, this study addresses the question of which material-specific properties must be considered in material modeling for an adequate deformation prediction. Characterization experiments were performed to gain a detailed understanding of the material mechanisms at the various process stages leading to residual stresses and warpage. The temperature dependence of stiffness was studied using DMA, the changes in length with temperature was studied using TMA, and the crystallization kinetics during cooling from the molten state and heating of a printed structure was studied using DSC at different cooling and heating rates. In the process phases up to annealing of the printed components, the strongly temperature-dependent stiffness and the reversible thermal expansion significantly determine the warpage that occurs. Crystallization effects can be neglected. During annealing, however, the influence of crystallization effects on volume and stiffness changes must be considered. Cold crystallization effects should be characterized on printed specimens. In addition, an irreversible change in volume occurs during annealing due to the molecular chains stretched by printing.

Acknowledgements

The authors gratefully acknowledge the Baden-Württemberg State Ministry of Science, Research and the Arts (MWK) for funding the project ‘Effiziente Prozessauslegung beim Verarbeiten von Polylactiden (PLA) in der Fused Filament Fabrication (FFF)’, and the German Research Foundation (DFG) for funding Prof. Kärger's Heisenberg Professorship (project no. 455807141).

References

[1] J. Butt, R. Bhaskar, Investigating the effects of annealing on the mechanical properties of FFF-printed thermoplastics, Journal of Manufacturing and Materials Processing 4 (2020) 1–20

[2] T. Tábi, I.E. Sajó, F. Szabó, A.S. Luyt, J.G. Kovács, Crystalline structure of annealed polylactic acid and its relation to processing, Express Polymer Letters 4 (2010) 659–668

[3] Y. Zhang, Y. Chou, Three-dimensional finite element analysis simulations of the fused deposition modelling process, Proceedings of the Institution of Mechanical Engineers, Part B: Journal of Engineering Manufacture 220 (2006) 1663–1671

[4] A.J. Favaloro, E. Barocio, B. Brenken, R.B. Pipes, E. Barocio, R.B. Pipes, Simulation of Polymeric Composites Additive Manufacturing using Abaqus, Dassault Systemes’ Science in the Age of Experience (2017) 103–114

[5] B. Brenken, E. Barocio, A. Favaloro, V. Kunc, R.B. Pipes, Development and validation of extrusion deposition additive manufacturing process simulations, Additive Manufacturing 25 (2019) 218–226

[6] A. Trofimov, J. Le Pavic, S. Pautard, D. Therriault, M. Lévesque, Experimentally validated modeling of the temperature distribution and the distortion during the Fused Filament Fabrication process, Additive Manufacturing 54 (2022) 102693

[7] S. Farah, D.G. Anderson, R. Langer, Physical and mechanical properties of PLA, and their functions in widespread applications — A comprehensive review, Advanced Drug Delivery Reviews 107 (2016) 367–392

[8] F.X. Espinach, S. Boufi, M. Delgado-Aguilar, F. Julián, P. Mutjé, J.A. Méndez, Composites from poly(lactic acid) and bleached chemical fibres: Thermal properties, Composites Part B: Engineering 134 (2018) 169–176

[9] J.S. Bergström, D. Hayman, An Overview of Mechanical Properties and Material Modeling of Polylactide (PLA) for Medical Applications, Annals of Biomedical Engineering 44 (2016) 330–340

[10] Z. Refaa, M. Boutaous, S. Xin, D.A. Siginer, Thermophysical analysis and modeling of the crystallization and melting behavior of PLA with talc: Kinetics and crystalline structures, Journal of Thermal Analysis and Calorimetry 128 (2017) 687–698

[11] S. Saeidlou, M.A. Huneault, H. Li, C.B. Park, Poly(lactic acid) crystallization, Progress in Polymer Science 37 (2012) 1657–1677

[12] M. Cristea, D. Ionita, M.M. Iftime, Dynamic mechanical analysis investigations of PLA-based renewable materials: How are they useful?, Materials 13 (2020) 1–24

[13] V. Srinivas, C.S.J. van Hooy-Corstjens, J.A.W. Harings, Correlating molecular and crystallization dynamics to macroscopic fusion and thermodynamic stability in fused deposition modeling; a model study on polylactides, Polymer 142 (2018) 348–355

[14] S. Wang, Y. Ma, Z. Deng, S. Zhang, J. Cai, Effects of fused deposition modeling process parameters on tensile, dynamic mechanical properties of 3D printed polylactic acid materials, Polymer Testing 86 (2020) 106483

[15] B. Huang, S.H. Masood, M. Nikzad, P.R. Venugopal, A. Arivazhagan, Dynamic mechanical properties of fused deposition modelling processed polyphenylsulfone material, American Journal of Engineering and Applied Sciences 9 (2015) 1–11

[16] O.A. Mohamed, S.H. Masood, J.L. Bhowmik, Experimental Investigations of Process Parameters Influence on Rheological Behavior and Dynamic Mechanical Properties of FDM Manufactured Parts, Materials and Manufacturing Processes 31 (2016) 1983–1994

[17] F. Frölich, L. Bechtloff, B.M. Scheuring, A.L. Heuer, F. Wittemann, L. Kärger, W. V. Liebig, Evaluation of mechanical properties characterization of additively manufactured components, Progress in Additive Manufacturing (2024)

[18] T. Yao, Z. Deng, K. Zhang, S. Li, A method to predict the ultimate tensile strength of 3D printing polylactic acid (PLA) materials with different printing orientations, Composites Part B: Engineering 163 (2019) 393–402

[19] J.A. Tröger, C. Steinweller, S. Hartmann, Identification, uncertainty quantification and validation of orthotropic material properties for additively manufactured polymers, Mechanics of Materials 197 (2024)

[20] Y. Zhao, Y. Chen, Y. Zhou, Novel mechanical models of tensile strength and elastic property of FDM AM PLA materials: Experimental and theoretical analyses, Materials and Design 181 (2019) 108089

[21] Forward AM Technologies GmbH. Technical Data Sheet Ultrafuse PLA. 2024

[22] E.W. Fischer, H.J. Sterzel, G. Wegner, Investigation of the structure of solution grown crystals of lactide copolymers by means of chemical reactions, Kolloid-Zeitschrift & Zeitschrift Für Polymere 251 (1973) 980–990. https://doi.org/10.1007/BF01498927